

Test of the universal local pseudopotential for the description of an inhomogeneous metal

Dmitriy S. Chekmarev, David W. Oxtoby, and Stuart A. Rice

Department of Chemistry and The James Franck Institute, The University of Chicago, Chicago, Illinois 60637

(Received 25 October 1999)

We present the results of a test of the adequacy of the recently proposed universal local electron-ion pseudopotential of Nogueira, Fiolhais, and Perdew [Phys. Rev. B **59**, 2570 (1999)] for the prediction of the structure of an inhomogeneous metal. The test is a comparison of the structure of the liquid-vapor interface of Ga predicted by self-consistent quantum Monte Carlo simulations with the observed structure. We find that the structure of the bulk liquid metal predicted using the universal local pseudopotential is in good agreement with experimental data if an effective temperature replaces the true temperature. However, the predicted structure of the liquid-vapor interface is only in qualitative agreement with experimental data. In particular, the longitudinal density distribution in the liquid-vapor interface predicted using the universal local pseudopotential is stratified, with a spacing of about one atomic diameter and a decay length of a few atomic diameters, features all of which are in qualitative agreement with observations. However, the amplitude of the predicted density oscillations is fivefold too large. Similar discrepancies are found when the longitudinal density distributions in the liquid-vapor interfaces of Sn and Pb predicted using the universal local pseudopotential are compared with those predicted using a nonlocal pseudopotential known to predict accurately the liquid-vapor interface structures of Ga and Hg. The results obtained imply that the *nonlocality* of the pseudopotential is critical to a correct description of the structure of an inhomogeneous metal.

I. INTRODUCTION

Our understanding of the structure and properties of inhomogeneous liquids is based on applications of density functional theory. Unfortunately, except for a few idealized models, a density functional analysis of an inhomogeneous liquid does not lead to an analytic representation of its structure and properties. Rather, after exploitation of approximations appropriate to the particular system, its structure and properties are obtained with one or another form of numerical analysis.

Consider, for example, the liquid-metal-vapor interface. The form of the effective interaction between ion cores in the inhomogeneous transition region between liquid metal and vapor is both density dependent and nonlocal, so it is not surprising that all current theoretical predictions of the character of the interface have been derived from self-consistent quantum Monte Carlo (MC) simulations. The analytical basis for the simulations is the density functional pseudopotential representation of the properties of an inhomogeneous metal.¹⁻⁴ The calculation of the system potential energy requires, as input, the electron density distribution in the interface; this distribution is obtained from the solution to the relevant Kohn-Sham equation.⁵ The effective pair potential is then used in a Monte Carlo simulation of the system properties. Since the local electron density changes when the ion cores are moved, the potential function must be recalculated after each Monte Carlo move. This procedure, when carried to convergence, generates self-consistent electron and ion core distributions for the metal. To date, the procedure described has been used to study the liquid-vapor interfaces of Na, K, Rb, Cs, Hg, Mg, Ga, Al, In, Tl, Sn, and Pb, and the dilute alloys Bi in Ga, In in Ga, Sn in Ga, and Pb in Ga. It is found that the density distribution along the normal to the liquid-vapor interface (called the longitudinal density distribution) has pronounced oscillations with a typical spacing of

about one atomic diameter; near the freezing point of the metal these oscillations penetrate three to four atomic diameters into the bulk liquid.^{1-4,6-20} On the vapor side of the interface the longitudinal density distribution falls rapidly to zero, with a scale length of a fraction of an atomic diameter. The difference between the structures of the liquid-vapor interfaces of simple metallic and nonmetallic liquids can be traced to the different forms of their potential energy functions. Specifically, the unique arrangement of atoms in the liquid-vapor interface of a simple metal is viewed as a consequence of a strong confinement of atoms in the interface, which has its origin in the substantial dependence of the system potential energy functional on the average valence electron density that varies across the interface. In general, there is very good agreement between the predicted^{3,15,18,20,21} and experimentally inferred^{6,8,9,11,22,23} longitudinal density distributions in the liquid-vapor interfaces of Hg, Ga, BiGa, InGa, SnGa, and PbGa.

The character and quality of the agreement between the results of the self-consistent quantum Monte Carlo simulations and the observed longitudinal density distributions in the liquid-vapor interfaces of these systems suggest that the extant theory can be used as a reliable predictor of the properties of other inhomogeneous liquid-metal systems. However, the calculations of the properties of the systems cited above utilize a sophisticated nonlocal representation of the electron-ion interactions and require very extensive and lengthy computations. Moreover, the formalism does not provide a simple conceptual picture of the elements of the interaction that are most important for the determination of the structure of the liquid-vapor interface of a metal. Thus there is no simple way of inferring the qualitative properties of a broad class of inhomogeneous metals and alloys from the knowledge of their nonlocal pseudopotentials.

It is clear that there would be considerable advantage in

having a description of inhomogeneous metals that permits prediction of the properties of the system using physical concepts based on the character of the atomic interaction. Since the pseudopotential representation of an electron-ion interaction is not unique,²⁴ we have considerable freedom in selecting its form, and we expect that a local pseudopotential will be more amenable to the construction of the wanted description of inhomogeneous metals than is a nonlocal pseudopotential. Recently, Nogueira, Fiolhais, and Perdew²⁵ have introduced a sophisticated local pseudopotential, called by them the universal local pseudopotential (ULP), that gives accurate predictions of the binding energies and elastic properties of many simple metals in their crystalline phases. In this paper we describe the results of self-consistent quantum Monte Carlo simulations of the liquid-vapor interfaces of Ga, Sn, and Pb. Our goal is to test the accuracy of the ULP when used to calculate the structure of the liquid-vapor interface of simple tri- and tetravalent metals; the measure of merit we use is, in the case of Ga, comparison with the experimentally inferred longitudinal density distribution in the liquid-vapor interface,^{6,8,9} and in the cases of Sn and Pb comparison with the longitudinal density distributions in the liquid-vapor interface predicted using a nonlocal pseudopotential [the energy independent model pseudopotential (EIMP) of Woo, Wang, and Matsuura²⁶] known to reproduce accurately those distributions for Ga and Hg.

The key results of the work reported below can be summarized as follows. The ULP correctly predicts the qualitative features of the stratification of the liquid-vapor interfaces of Ga, Sn, and Pb. However, the modulation of the longitudinal density distribution supported by the ULP is much greater than that found experimentally, and also much greater than that found using the nonlocal EIMP pseudopotential. The results clearly imply that, despite its utility for calculation of the properties of homogeneous metals, the ULP is unsatisfactory for quantitative prediction of the structure of an inhomogeneous metal.

II. DETAILS OF SIMULATIONS

The theoretical basis for the work reported in this paper has been described in our previous reports.^{1-3,19} The self-consistent quantum MC simulations are based on the density functional pseudopotential theory of inhomogeneous metals in the form first adopted by D'Evelyn and Rice^{1,12} and later modified by Harris, Gryko, and Rice.² The essence of any pseudopotential theory^{27,28} lies in the replacement of the strong direct interaction between the delocalized electrons and the ions by an effective, small in magnitude and, in principle, nonlocal pseudopotential that accounts for the requirement that the states of the delocalized electrons are orthogonal to the states of the ion core electrons. The total system energy is then calculated as the sum of the zero-order energy associated with the immersion of a degenerate electron gas in a nonuniform continuum distribution of positive charge (an inhomogeneous jellium) and the first- and second-order perturbation theory corrections for the interaction between the discrete ions and the electrons. To second order in perturbation theory, the Hamiltonian of an arbitrary configuration of N metallic ions and NZ sp -valence electrons is then given by

$$H = \sum_{i=1}^N \frac{\mathbf{p}_i^2}{2m} + U_0(\rho_0(\mathbf{r}), n_{el}(\mathbf{r})) + \sum_{i < j} V_{\text{eff}}(\mathbf{R}_i, \mathbf{R}_j; n_{el}^{\text{LDA}}(r)) \quad (1)$$

where \mathbf{p}_i is the momentum of the i th atom with mass m , $V_{\text{eff}}(\mathbf{R}_i, \mathbf{R}_j; n_{el}^{\text{LDA}}(r))$ is the effective pair potential (evaluated in the local density approximation) between ions i and j located at \mathbf{R}_i and \mathbf{R}_j , respectively, and $\rho_0(\mathbf{r})$ and $n_{el}(\mathbf{r})$ are the corresponding reference jellium and electron densities. The functional U_0 is a structure-independent contribution to the energy, which is, however, dependent on the electron and jellium densities. In the following discussion, we use atomic units for length [1 a.u. = 1 a_0 (Bohr radius) = 0.529 177 Å] and energy (1 a.u. = 2 Ry = 27.21 eV). In some of the analysis described below it is convenient to use the volume per atom, $\Omega = \rho^{-1}$.

For local model pseudopotentials, the effective pair interaction takes the form

$$V_{\text{eff}}(R; n_{el}^{\text{LDA}}) = \frac{Z^2}{R} \left(1 - \frac{2}{\pi} \int_0^\infty \frac{F_N(q) \sin(qR)}{q} dq \right), \quad (2)$$

where the first term is the direct Coulomb repulsion between ions of charge Z and the second term is the second-order pseudopotential contribution to the pair interaction potential. The structure-independent energy U_0 is a function of the electron density $n_{el}(\mathbf{r})$ and the positive (reference) charge density $\rho_0(\mathbf{r})$ but does not depend explicitly on the positions of ions. $U_0(\rho_0(\mathbf{r}), n_{el}(\mathbf{r}))$, which is responsible for by far the largest contribution to the system energy (about 95%), can be represented as the sum of the kinetic energy, the electrostatic energy (which arises from the lack of coincidence of the electron and ion density distributions in the liquid-vapor transition zone), the exchange-correlation energy, and the electron-ion pseudopotential interaction,

$$U_0(\rho_0(\mathbf{r}), n_{el}(\mathbf{r})) = E_{\text{kin}} + E_{\text{es}} + E_{\text{xc}} + E_{\text{ps}}. \quad (3)$$

The electronic kinetic energy E_{kin} can be calculated by solving directly the self-consistent Kohn-Sham equation.²⁹

The last term in Eq. (3), the electron-ion pseudopotential contribution, must be discussed in more detail both because of the crucial role it plays in determining the structure of the liquid-vapor interface and because, unlike all other terms in Eq. (3), it assumes different forms depending on whether a local or nonlocal pseudopotential is used. In the local density approximation, this term can be written (the system is assumed to have a planar interface) as

$$E_{\text{ps}} = 2A \int_0^\infty dz \rho_0(z) \epsilon_{\text{ps}}(n_{el}(z)), \quad (4)$$

where ϵ_{ps} has the following form when a local pseudopotential is used:

$$\epsilon_{\text{ps}} = 3 \int_0^1 f_{\text{ir}}(\eta, \eta) \eta^2 d\eta - \left[\frac{2\pi Z^2}{\Omega} \lim_{q \rightarrow 0} \frac{1 - F_N(q)}{q^2} + \frac{Z^2}{\pi} \int_0^\infty F_N(q) dq \right] + f_{\text{corr}}. \quad (5)$$

In Eq. (5), $r_s = [(3/4\pi)n_{el}^{-1}]^{1/3}$ is the radius of a sphere containing on average one electron, $\eta = k/k_F$, and $f_{lr}(\eta, \eta) = Z\langle k|w_{nc}|k\rangle$ is the diagonal matrix element of the non-Coulombic part of the bare pseudopotential. The first term in Eq. (5) is the first-order correction to the system energy from the electron-ion pseudopotential. It is not influenced by screening since screening is merely a redistribution of the electron density (as long as the total charge is conserved) and, therefore, has no effect on average values. The next two terms (in square brackets) are second-order corrections. In order to compensate for the failure of the bare pseudopotential to ensure the mechanical stability of the model system, as well as to yield the correct value for the heat of vaporization at the experimental bulk density, it is necessary to introduce corrections to the structure independent energy.^{2,19,20} These empirical corrections are embedded in the last contribution to ϵ_{ps} in Eq. (5).

In Eqs. (2) and (5) the key ingredient is the normalized energy-wave-number characteristic $F_N(q)$, which is quadratic in the electron-ion pseudopotential and can be written (again for a local pseudopotential) as

$$F_N(q) = \left(-\frac{q^2\Omega}{2\pi Z^2} \right) \frac{\Omega q^2}{8\pi} \left(\frac{1 - \epsilon^H(q)}{\bar{\epsilon}(q)} \right) |\omega_{bare}(q)|^2, \quad (6)$$

where $\omega_{bare}(q)$ is the Fourier transform of the bare pseudopotential and $\epsilon^H(q)$ is the static dielectric function of the electron gas calculated in the random phase approximation (no exchange and correlation contribution). The modified dielectric function, $\bar{\epsilon}(q)$, with exchange and correlation included, is related to $\epsilon^H(q)$ by¹

$$\bar{\epsilon}(q) = 1 + [\epsilon^H(q) - 1][1 - G(q)], \quad (7)$$

where $G(q)$ is the local-field corrector.^{24,28} Hence, for any given inhomogeneous metal the problem is fully specified by the choice of an appropriate form of the pseudopotential $\omega_{bare}(r)$, the local-field function $G(q)$, and the parametric form of the reference jellium profile $\rho_0(\mathbf{r})$.

In the present work we employ the universal local electron-ion pseudopotential due to Nogueira, Fiolhais, and Perdew.²⁵ This model potential derives from a family of local pseudopotentials known as evanescent core (EC) model potentials³⁰ that have been designed specifically for use with a second-order nonrelativistic perturbation treatment of simple metals in the local density approximation. By virtue of its construction, the ULP and its derivatives are continuous throughout the space (this smoothness ensures better convergence properties in the reciprocal space over lattice vectors), and the evanescence of the core repulsion is naturally incorporated in the form described. The real-space representation of the evanescent core pseudopotential is given by³⁰

$$\begin{aligned} \omega_{EC}(r) = & -\frac{Z}{r} \{1 - [1 + \beta(r/R_{EC})] \exp(-\alpha r/R_{EC})\} \\ & + \frac{Z}{R_{EC}} A \exp(-r/R_{EC}), \end{aligned} \quad (8)$$

where R_{EC} is the core decay length and $\alpha > 0$. In principle, this representation contains four independent parameters

R_{EC} , A , α , and β , but two of them, namely, A and β , can be determined in terms of α by imposing the analyticity condition (cusp-free condition) at $r=0$. The remaining two parameters are fixed by requiring that the total energy per electron of a solid metal calculated to second order in perturbation theory (within the local density approximation) be a minimum at the equilibrium value of the Wigner-Seitz radius, and that the calculated bulk modulus reproduce the result of the stabilized jellium model (effective valence 1).²⁵ With these restrictions imposed the model pseudopotential contains no adjustable parameters.

In Fourier space, the matrix element of $\omega_{EC}(r)$, the form factor, can be expressed analytically,³⁰ which in turn allows an analytical expression for $F_N(q)$ to be obtained from Eq. (6). The EC pseudopotentials have been tested extensively with respect to predictions of lattice dynamics, elastic moduli, liquid-metal resistivities, binding energies,^{25,30,31} and the pair correlation functions of bulk liquid alkali metals.³² In all cases good agreement with available experimental data is obtained. It is important to emphasize that the descriptor ‘‘universal’’ in the designation of the ULP means that the pseudopotential has parameters determined solely by the equilibrium electron density and the valence.

It is well known²⁸ that the shape of a pair interaction potential in metals may depend crucially on the choice of the effective-field function $G(q)$. For reasons of convenience, we chose to work with the local-field function proposed by Ichimaru and Utsumi³³ [$G_{IU}(q)$]; this function satisfies the electron-gas sum rules, and its parametrized form is particularly suitable for use in computer simulations. The parameters of the ULP in a given density range for a certain valence were found²⁵ from the values of the binding energy and bulk modulus, both calculated to second order in perturbation theory and employing the local density approximation local-field correction. The replacement of $G_{LDA}(q)$ by $G_{IU}(q)$ in simulations is likely to have a minor effect on the interface structure. This assertion derives from the well-established fact²⁸ that the deviations between various forms of $G(q)$ that have the most profound physical consequences are in the region $1.5k_F < q < 2.0k_F$, where $G_{LDA}(q)$ and $G_{IU}(q)$ do not differ significantly. The small- q limits are very similar for different $G(q)$'s, and the large- q behaviors are not critical since the polarizability decreases rapidly for $q > 2.0k_F$. In Fig. 1, we show the effective pair interaction potentials for Pb calculated using $G_{LDA}(q)$ and $G_{IU}(q)$, respectively. Clearly, the difference in the shapes of the two potentials is very small.

The only remaining quantity one needs to specify to complete the description of an inhomogeneous liquid metal according to the formalism outlined above is the reference positive density distribution $\rho_0(\mathbf{r})$. In the case of a planar liquid-vapor interface, ρ_0 can be modeled by²

$$\rho_0(z, z_0, \beta) = \frac{\rho_{bulk}}{1 + \exp\left(\frac{|z| - z_0}{\beta}\right)}, \quad (9)$$

where z_0 is the position of the Gibbs dividing surface and β characterizes the width of the inhomogeneous region of the jellium profile. This distribution is properly normalized by setting

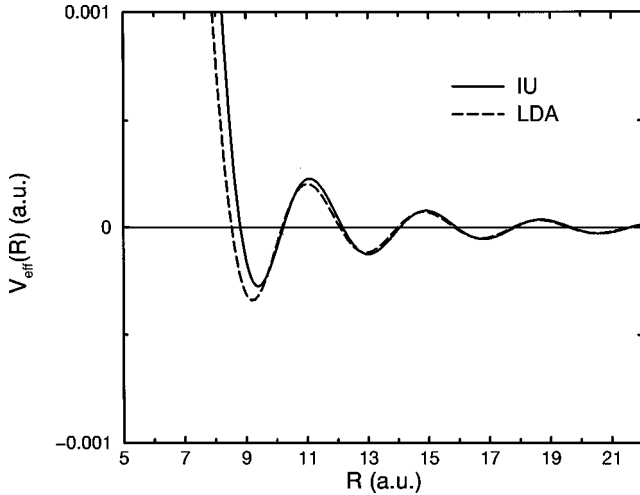


FIG. 1. Effective pair potential for Pb ($r_s=2.3$): with Ichimaru-Utsumi (IU) local-field function (—), with LDA local-field function (---).

$$\rho_{bulk} = \frac{N}{2A \left\{ z_0 + \beta \ln \left[1 + \exp \left(-\frac{z_0}{\beta} \right) \right] \right\}}, \quad (10)$$

where N is the total number of atoms in the slab and A is the area of one free face of the slab. For most situations encountered in practice during the simulation run, Eq. (10) can be safely replaced by a simpler expression, namely, $\rho_{bulk} = N/2Az_0$ (note that since z_0 changes at each simulation step the value of ρ_{bulk} may deviate from the initially set experimental bulk number density).

Given the form of the pseudopotential, the self-consistent quantum MC simulations were carried out as follows. The model system was a slab with dimensions $L_0 \times L_0 \times 2L_0$ containing 1000 ions. The slab was subject to periodic boundary conditions in the x and y directions and had free surfaces in the $\pm z$ directions (across the liquid-vapor transition zone). For convenience, periodic boundary conditions were also applied in the $\pm z$ directions, but at distances very far from the the Gibbs dividing surfaces. This convenience does not influence our results.¹⁹

The center of mass of the simulation sample was positioned at $z=0$, which is the location of the origin of the coordinates. The linear dimension of the simulation box, L_0 , was chosen such that the initial density of the slab is equal to the known bulk density ρ_{bulk} at the temperature of interest. The simulation slab is about 16 layers deep (each roughly one atomic diameter in thickness), 8 layers for each half.

The simulations were started by placing the particles at random positions within the boundaries of the slab. Initial configurations that have ion-core-ion-core overlaps are eliminated by a force-biased Monte Carlo simulation with periodic boundary conditions in all directions, using a scaled Lennard-Jones potential for the ion cores. In the course of a simulation ions are moved sequentially, one at a time, and the new configurations are accepted or rejected according to the standard procedure (Metropolis scheme³⁴) by consulting the appropriate Boltzmann factors. About 46×10^6 configurations were generated for each metal, from which the last 12×10^6 were used in collecting the final statistics.

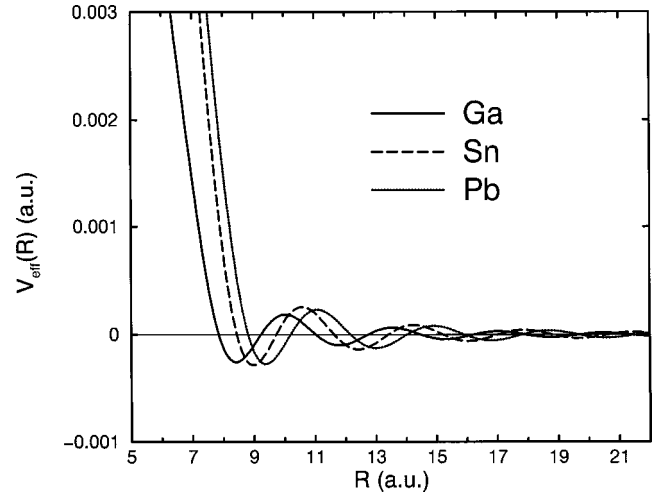


FIG. 2. Effective pair potentials for Ga at $r_s=2.18$ (—), Sn at $r_s=2.22$ (---), and Pb at $r_s=2.3$ (-·-·-).

For each instantaneous ionic configuration the reference jellium parameters z_0 and β were determined using a weighted least-squares fit of the discrete moments of the ion distribution to the continuous moments of $\rho(z, z_0, \beta)$.^{2,19} Then, using this jellium distribution, the corresponding electron density distribution was obtained from the solution of the pertinent Kohn-Sham equation.^{4,19,29}

For each ionic configuration the corresponding electron density profile is a function of z , z_0 , and β , and the structure-independent energy U_0 is a function of the width parameter β and the liquid density ρ_{bulk} . To simplify the computational scheme we adopted the following approximate form for U_0 :

$$U_0[\beta, \rho_{bulk}] \approx Nu_0[\rho_{bulk}] + 2A\sigma_U[\beta], \quad (11)$$

where $u_0[\rho_{bulk}]$ is the structure independent energy per particle of a homogeneous system with density ρ_{bulk} , and $\sigma_U[\beta]$ is the surface energy (per unit area) of the reference jellium distribution represented by Eq. (9). This approximation proved adequate for sufficiently large systems (~ 1000 atoms).¹⁹ To obtain the longitudinal ion density distribution, a histogram of particle positions relative to the position of the center of mass of the slab was compiled during the course of the simulation run. The density profiles from opposite halves of the slab were then averaged. The in-plane structure of the model system is described by the transverse pair correlation function, which we have calculated for thin sections sliced parallel to the interface.^{2,19}

III. RESULTS AND DISCUSSION

We have tested the accuracy of the ULP with respect to prediction of the pair correlation functions of liquid Ga, Sn, and Pb. For these three-dimensional (3D) bulk MC simulations we used a simulation box that contains 512 particles and employed periodic boundary conditions in the x , y , and z directions. The effective pair interaction potentials were calculated for densities corresponding to the equilibrium solid-state structures, namely $r_s=2.18$ (rhombohedral) for Ga, $r_s=2.22$ (tetragonal) for Sn, and $r_s=2.3$ (fcc) for Pb. The resultant potentials are displayed in Fig. 2. We note that the changes in density that occur with increasing T produce

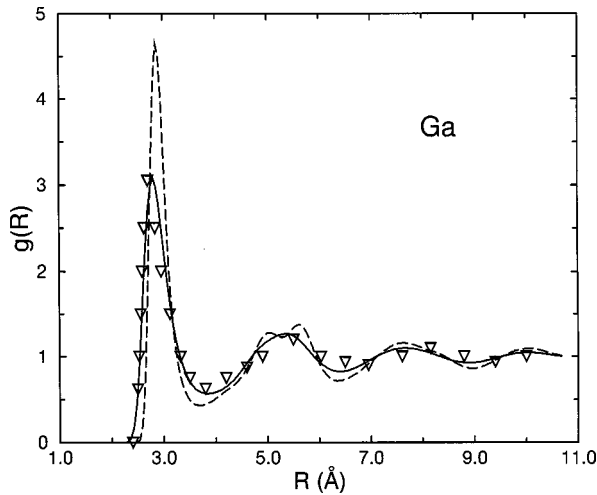


FIG. 3. Pair correlation function for bulk liquid Ga: MC at $T_{sim} = 1173$ K and $\rho_{bulk} = 0.0525$ (atoms/Å³) (—), MC at $T_{sim} = 330$ K (-----), and experiment (Ref. 35) at $T_{expt} = 326$ K ($\nabla\nabla\nabla$).

rather small differences in the shape of the effective pair potential for temperatures not too far from the melting point. It was found that if the simulations were carried out at the experimental values of the melting density and melting temperature,^{35,36} the predicted pair correlation functions do not agree well with the experimentally determined functions. The discrepancies found are largely in the magnitudes of the peaks and valleys of $g(R)$ but not in their positions, so that the simulated $g(R)$'s resemble those of strongly undercooled liquids. We infer, then, that the source of these deviations is the exaggerated depth of the first potential well of the ULP and the appreciable amplitudes of the tail oscillations; together these features of the ULP define the “stiffness” of the liquid structure against variation of the temperature. For each of the metals studied, by fixing the liquid density at the experimental value at the melting point and raising the temperature, it is possible to find a temperature at which the deviation between the calculated and observed bulk liquid pair correlation functions is removed. Comparisons of the results of the simulations and the available experimental data are shown in Figs. 3, 4, and 5 for Ga, Sn, and Pb, respectively. The same densities and temperatures were then used in the simulations of the respective liquid-vapor interfaces of these metals.

Consider, now, the shapes of the pair potentials displayed in Fig. 2. These potentials look very similar because, within the framework of the ULP formalism, the key defining parameters, namely, the equilibrium electron densities and the valences, are very similar in value. For small ion-core-ion-core separations these potentials have strongly repulsive cores, and at slightly larger separations they have attractive wells; the attractive well can be very shallow for some metals.^{17,20,37,39} As the ion-core-ion-core distance grows, the potential displays Friedel oscillations that decay as $\cos(2k_F R)/(2k_F R)^3$. For a local pseudopotential, the amplitude of these oscillations is controlled by the magnitude of the pseudopotential matrix element $|\omega(q)|^2$ evaluated at $q = 2k_F$. Comparison between the pair potentials for Ga, Sn, and Pb obtained with the ULP and the nonlocal EIMP treatment of Zhao *et al.*³ and Rice and Zhao⁴² reveals that the ULP model predicts quite prominent Friedel oscillations for

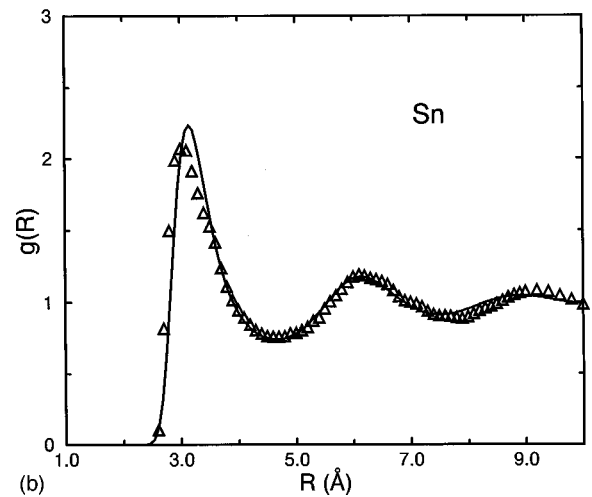
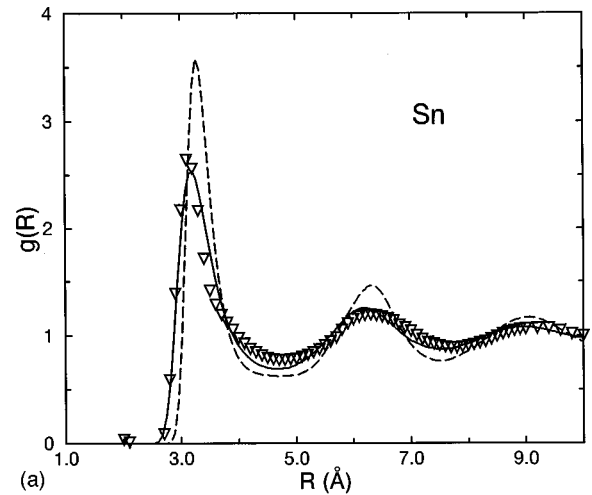


FIG. 4. Pair correlation function for bulk liquid Sn: (a) MC at $T_{sim} = 1900$ K and $\rho_{bulk} = 0.0346$ (atoms/Å³) (—), MC at $T_{expt} = 600$ K (-----) and experiment (Ref. 36) at $T_{expt} = 573$ K ($\nabla\nabla\nabla$); (b) MC at $T_{sim} = 3000$ K and $\rho_{bulk} = 0.0337$ (atoms/Å³) (—), experiment (Ref. 36) at $T_{expt} = 973$ K ($\Delta\Delta\Delta$).

each of Ga, Sn, and Pb, signaling large values of the on-Fermi-sphere pseudopotential matrix elements. In contrast, the nonlocal EIMP model potential oscillations are strongly damped, meaning that the matrix element $\langle \mathbf{k} + \mathbf{q} | w | \mathbf{k} \rangle$ tends to be small around $q = 2k_F$. We note again that our analysis is developed from second-order perturbation theory, and it depends on the smallness of the pseudopotential. Then it is immediately clear that when a local pseudopotential is used the error associated with the truncation of the perturbation expansion at second order, which amounts to neglecting three-body and higher contributions, may not be satisfactory. The situation can be partially ameliorated by inclusion of the correction term f_{corr} [in Eq. (5)], which serves the purpose of projecting higher-order terms back into “effective” lower-order terms. Nonetheless, as will be discussed in a moment, the procedure used to determine the correction term for a specific case is not without some internal difficulties. On these grounds, it seems likely that a quantitative description of the structure of the liquid-vapor interface of a heavy polyvalent metal will require the use of a nonlocal pseudopotential. This expectation concerning the importance of the use of nonlocal pseudopotentials for heavy polyvalent metals

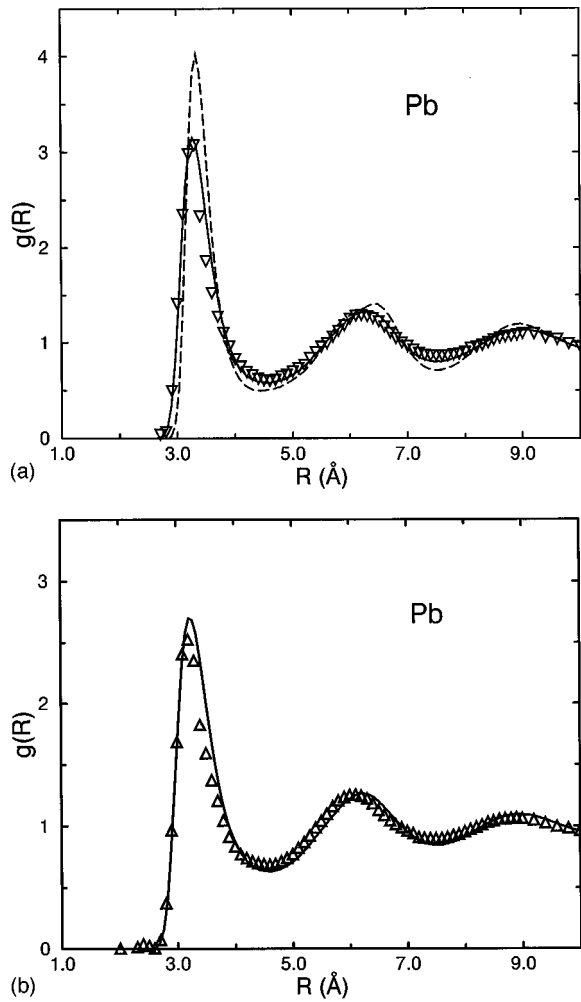


FIG. 5. Pair correlation function for bulk liquid Pb: (a) MC at $T_{sim} = 1350$ K and $\rho_{bulk} = 0.0332$ (atoms/Å³) (—), MC at $T_{expt} = 650$ K (----) and experiment (Ref. 36) at $T_{expt} = 613$ K ($\nabla\nabla\nabla$); (b) MC at $T_{sim} = 2200$ K and $\rho_{bulk} = 0.0321$ (atoms/Å³) (—), experiment (Ref. 36) at $T_{expt} = 1023$ K ($\triangle\triangle\triangle$).

has previously been voiced by Jank and Hafner^{37,38} on the basis of a scrupulous analysis of the atomic and electronic structures of bulk liquid Ga, Sn, and Pb.

We now turn to a description of the results of simulation studies of the liquid-vapor interfaces of Ga, Sn, and Pb using the ULP model. In Fig. 6 we show the dependence of the surface energy per unit area σ_U [refer to Eq. (11)] on the reference profile width parameter β calculated for Ga at $T_{sim} = 1173$ K, for Sn at $T_{sim} = 3000$ K and for Pb at $T_{sim} = 2200$ K. The shapes of the curves resemble those for simple metals.² The liquid-vapor interface widths should be close to the values corresponding to the minima in the σ_U versus β curve. From Fig. 6 $\beta_{min} \approx 0.20$ a.u. for Ga and $\beta_{min} \approx 0.15$ a.u. for Sn and Pb. These values of β imply that all three metals have rather narrow liquid-vapor interfaces.

The structural feature of most interest to us is the singlet ion density distribution across the liquid-vapor interface. In this regard, the most stringent test of the accuracy of the ULP is the direct comparison of predicted and observed longitudinal density distributions; of the liquids studied in this paper, these data are available only for Ga.^{6,8} A comparison of predicted and observed longitudinal density distributions

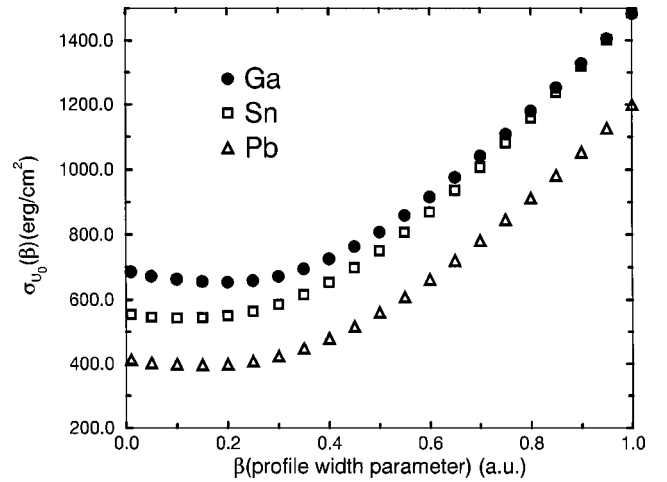


FIG. 6. Surface energy per unit area $\sigma_U(\beta)$ calculated for Ga ($\bullet\bullet\bullet$) at $T_{sim} = 1173$ K, Sn ($\square\square\square$) at $T_{sim} = 3000$ K, and Pb ($\triangle\triangle\triangle$) at $T_{sim} = 2200$ K.

is provided in Fig. 7. Clearly, the ULP model reproduces the qualitative features of the experimentally determined density profile: the interlayer spacing is about one atomic diameter and the layering decay length is about four atomic diameters. Nonetheless, the ULP model predicts much larger amplitude density oscillations than are observed. The nonlocal EIMP model³ prediction of the longitudinal density distribution is in much better agreement with experiment (see Fig. 10 of Ref. 3).

In Figs. 8 and 9 we compare the longitudinal density distributions in the liquid-vapor interfaces of Sn and Pb predicted using the ULP with those predicted using the nonlocal EIMP.⁴² Again, we find that the predicted interlayer spacing is about one atomic diameter and that the ion-core density oscillations penetrate into the fluid for about 2 to 3 atomic diameters. And, as in the case of liquid Ga, the ULP generates exceedingly large amplitude oscillations in the longitudinal density distribution.

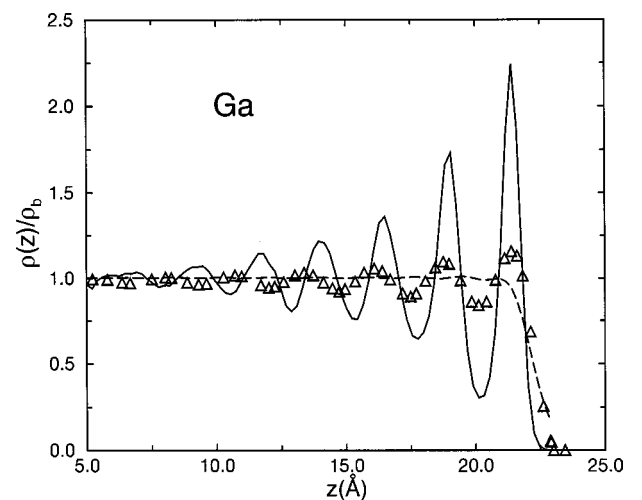


FIG. 7. Comparison of the longitudinal density distribution in the liquid-vapor interface of Ga calculated using the ULP model (current study at $T_{sim} = 1173$ K): ion density (—), electron density (---), and experimental data of Regan *et al.* (Ref. 8) at $T = 22^\circ\text{C}$ ($\triangle\triangle\triangle$).

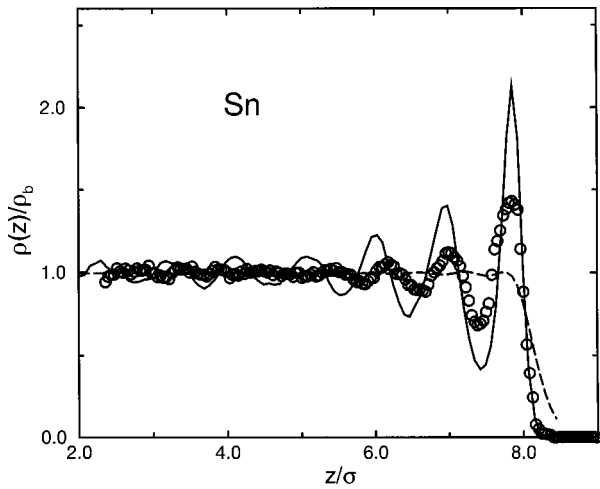


FIG. 8. Comparison of the longitudinal density distribution in the liquid-vapor interface of Sn calculated using the ULP model (current study at $T_{sim} = 3000$ K): ion density (—), electron density (---), and the ion density obtained using the nonlocal EIMP model of Ref. 42 (○○○).

Finally, we examine the transverse (in-plane) structure in the liquid-vapor interfaces of Ga, Sn, and Pb. We have calculated the transverse pair correlation functions in the liquid-vapor interfaces of these metals from histograms of the separations of all pairs of particles in a series of thin strata parallel to the interface. For each metal, we display in Fig. 10 the transverse pair distribution functions computed for the outermost layer, corresponding to the region that encloses the first high density peak in $\rho(z)$, the second layer, and the experimentally determined^{35,36} bulk liquid $g(R)$. Despite the oscillatory variation in density across the liquid-vapor interface, the transverse pair correlation function is always very nearly the same as that of the bulk liquid. The insensitivity of the transverse pair distribution function to the point local density is successfully accounted for by the Fischer-Methfessel⁴⁰ extended local density approximation,

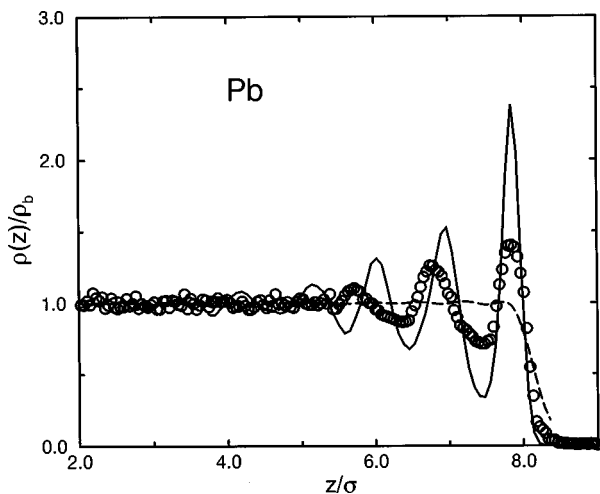


FIG. 9. Comparison of the longitudinal density distribution in the liquid-vapor interface of Pb calculated using the ULP model (current study at $T_{sim} = 2200$ K): ion density (—), electron density (---), and the ion density obtained using the nonlocal EIMP model of Ref. 42 (○○○).

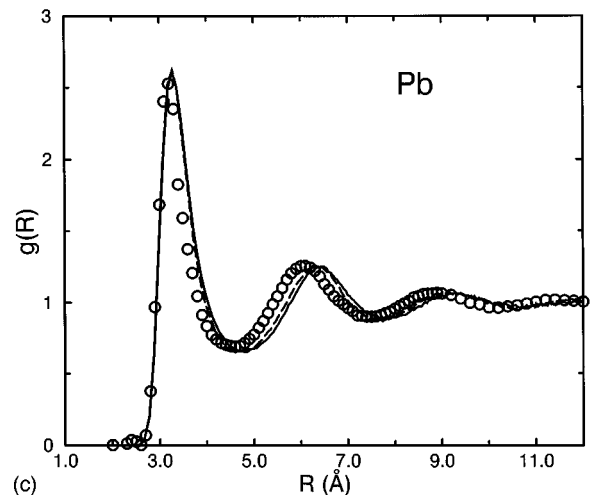
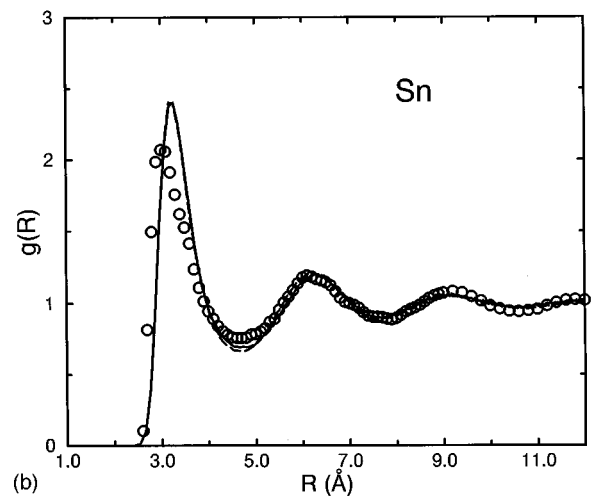
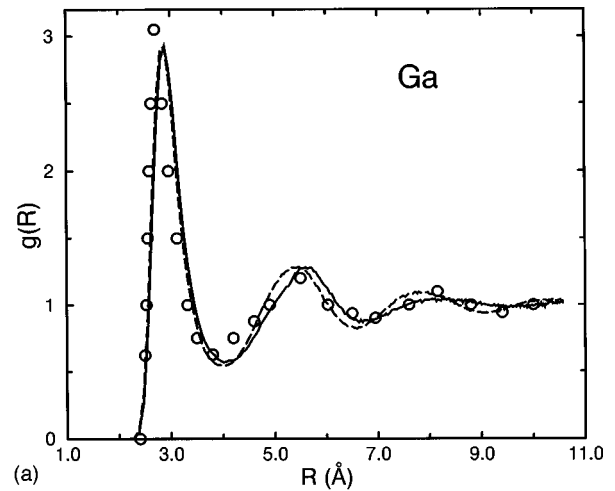


FIG. 10. Transverse pair correlation functions for selected layers from the liquid-vapor interface of (a) Ga, (b) Sn, and (c) Pb. Outermost layer (—), second layer (---), and experiment (Refs. 35 and 36) (○○○). Temperatures are the same as in Figs. 3–5.

which states that the in-plane structure is determined by an effective density that is defined by averaging the point density in a volume element that has linear dimensions comparable to an atomic diameter. The simulation results reported in this paper are fully consistent with the results of previous MC simulation studies of trivalent metals.¹⁷

Given the inherent complexity of the problem, pinpointing how the local pseudopotential errs in the description of the interactions in a heavy polyvalent metal is nontrivial. The following speculations seem pertinent.

It is currently believed that the temperature dependence of the widths of the peaks in the longitudinal density distribution is adequately described by capillary wave theory.^{3,8,20,41} The long-wavelength cutoff in the spectrum of capillary wave excitations is set by the size of the sample.^{7-9,20} Since the simulation sample is very small, the widths of the peaks in the longitudinal density distribution are underestimated, and, correspondingly, the peak amplitudes are overestimated. Since the surface energy (which is close to but not identical to the surface tension) calculated with the local pseudopotential model is larger than that calculated with the nonlocal pseudopotential, the structure in the longitudinal density distribution calculated with the former is exaggerated relative to that calculated with the latter. In this connection, it is worthwhile noting that the calculated longitudinal density profile in the liquid-vapor interface of Ga displayed in Fig. 7 resembles closely the extrapolated “zero-temperature intrinsic longitudinal density profile” determined in the experimental study of Regan *et al.*⁸ (see inset on Fig. 2 of Ref. 8). This observation suggests that the ULP has an attractive well that is too deep and too narrow, and that the oscillations in the tail of the potential are too strong. The simulations of the bulk liquid structure using the ULP support this conjecture. For the metals considered in this paper, in order to achieve

good agreement between the simulated and measured pair correlation functions, we found it necessary to carry out the simulations at unphysically large temperatures, whereas when the nonlocal EIMP pseudopotential is used agreement is achieved with simulation temperatures very close to those at which the experimental data were collected.^{3,42}

Another possible source of error in the ULP is associated with the correction term f_{corr} in Eq. (5). This term is introduced to remove the large negative value of pressure that is generated by the other terms in Eq. (5).^{28,32,43} In general, the magnitude of f_{corr} is large for primitive local pseudopotential models. If f_{corr} is ignored, the resultant oscillations in the longitudinal density profile are strongly enhanced.¹⁹ Since the routine to determine f_{corr} is designed to work in the vicinity of the equilibrium bulk density, as the simulations proceed the changes in the bulk density (see simulation procedure for details) may exceed the range for which the calculated correction is valid. We conclude that, useful as they are for the calculation of the properties of crystalline metals, local pseudopotentials are not sufficiently accurate to provide other than qualitative predictions of the structure of the liquid-vapor interface of a metal.

ACKNOWLEDGMENTS

We wish to thank Dr. Meishan Zhao for his assistance. This work has been supported by a grant from the National Science Foundation.

-
- ¹M. P. D’Evelyn and S. A. Rice, *J. Chem. Phys.* **78**, 5225 (1983).
²J. G. Harris, J. Gryko, and S. A. Rice, *J. Chem. Phys.* **87**, 3069 (1987).
³M. Zhao, D. Chekmarev, Z. Cai, and S. A. Rice, *Phys. Rev. E* **56**, 7033 (1997).
⁴D. S. Chekmarev, Ph.D. thesis, The University of Chicago (1999).
⁵P. Hohenberg and W. Kohn, *Phys. Rev.* **136**, B864 (1964); W. Kohn and L. J. Sham, *Phys. Rev.* **140**, A1133 (1965).
⁶M. J. Regan, E. H. Kawamoto, S. Lee, P. S. Pershan, N. Maskil, M. Deutsch, O. M. Magnussen, and B. M. Ocko, *Phys. Rev. Lett.* **75**, 2498 (1995).
⁷O. M. Magnussen, B. M. Ocko, M. J. Regan, K. Penanen, P. S. Pershan, and M. Deutsch, *Phys. Rev. Lett.* **74**, 4444 (1995).
⁸M. J. Regan, P. S. Pershan, O. M. Magnussen, B. M. Ocko, M. Deutsch, and L. E. Berman, *Phys. Rev. B* **54**, 9730 (1996).
⁹M. J. Regan, P. S. Pershan, O. M. Magnussen, B. M. Ocko, M. Deutsch, and L. E. Berman, *Phys. Rev. B* **55**, 15 874 (1997).
¹⁰M. J. Regan, H. C. Tostmann, P. S. Pershan, O. M. Magnussen, E. DiMasi, B. M. Ocko, and M. Deutsch, *Phys. Rev. B* **55**, 10 786 (1997).
¹¹N. Lei, Z. Huang, and S. A. Rice, *J. Chem. Phys.* **104**, 4802 (1996).
¹²M. P. D’Evelyn and S. A. Rice, *J. Chem. Phys.* **78**, 5081 (1983).
¹³J. G. Harris, J. Gryko, and S. A. Rice, *J. Stat. Phys.* **48**, 1109 (1987).
¹⁴A. Gomez and S. A. Rice, *J. Chem. Phys.* **101**, 8094 (1994).
¹⁵M. Zhao, D. Chekmarev, and S. A. Rice, *J. Chem. Phys.* **108**, 5055 (1998).
¹⁶S. A. Rice, M. Zhao, and D. Chekmarev, in *Microscopic Simulation of Interfacial Phenomena in Solids and Liquids*, edited by S. R. Phillpot, P. D. Bristowe, D. G. Stroud, and J. R. Smith (The Materials Research Society, Pittsburgh, PA, 1998), pp. 3–14.
¹⁷M. Zhao, D. Chekmarev, and S. A. Rice, *J. Chem. Phys.* **109**, 1959 (1998).
¹⁸S. A. Rice and M. Zhao, *Phys. Rev. B* **57**, 13 501 (1998).
¹⁹D. Chekmarev, M. Zhao, and S. A. Rice, *J. Chem. Phys.* **109**, 768 (1998).
²⁰D. S. Chekmarev, M. Zhao, and S. A. Rice, *Phys. Rev. E* **59**, 479 (1999); **59**, 6206 (1999).
²¹M. Zhao and S. A. Rice, *J. Chem. Phys.* **111**, 2181 (1999).
²²E. DiMasi, H. Tostmann, B. Ocko, P. S. Pershan, and M. Deutsch, *Phys. Rev. B* **58**, R13 419 (1998).
²³N. Lei, Z. Huang, and S. A. Rice, *J. Chem. Phys.* **107**, 4051 (1997).
²⁴M. Shimoji, *Liquid Metals: An Introduction to the Physics and Chemistry of Metals in the Liquid State* (Academic Press, New York, 1977).
²⁵F. Nogueira, C. Fiolhais, and J. P. Perdew, *Phys. Rev. B* **59**, 2570 (1999).
²⁶C. H. Woo, S. Wang, and M. Matsuura, *J. Phys. F: Met. Phys.* **5**, 1836 (1975); M. Matsuura, C. H. Woo, and S. Wang, *ibid.* **5**, 1849 (1975); S. Wang, S. K. Lai, and C. B. So, *ibid.* **10**, 445 (1980), and references therein.
²⁷W. A. Harrison, *Pseudopotentials in the Theory of Metals* (Benjamin, New York, 1966); W. H. Young, *Rep. Prog. Phys.* **55**, 1769 (1992).
²⁸J. Hafner, *From Hamiltonians to Phase Diagrams* (Springer-Verlag, Berlin, 1987).

- ²⁹A. G. Eguiluz, D. A. Campbell, A. A. Maradudin, and R. F. Wallis, Phys. Rev. B **30**, 5449 (1984).
- ³⁰C. Fiolhais, J. P. Perdew, S. Q. Armster, J. M. MacLaren, and M. Brajczewska Phys. Rev. B **51**, 14 001 (1995).
- ³¹L. Pollack, J. P. Perdew, J. He, M. Marques, F. Nogueira, and C. Fiolhais, Phys. Rev. B **55**, 15 544 (1997).
- ³²M. Boulahbak, N. Jakse, J.-F. Wax, and J.-L. Bretonnet, J. Chem. Phys. **108**, 2111 (1998).
- ³³S. Ichimaru and K. Utsumi, Phys. Rev. B **24**, 7385 (1981).
- ³⁴N. Metropolis, A. W. Rosenbluth, M. N. Rosenbluth, A. M. Teller, and E. Teller, J. Chem. Phys. **21**, 1087 (1953).
- ³⁵M. C. Bellissent-Funel, P. Chieux, D. Levesque, and J. J. Weis, Phys. Rev. A **39**, 6310 (1989).
- ³⁶Y. Waseda, *The Structure of Non-Crystalline Materials—Liquids and Amorphous Solids* (McGraw-Hill, New York, 1980).
- ³⁷W. Jank and J. Hafner, Phys. Rev. B **41**, 1497 (1990).
- ³⁸J. Hafner and W. Jank, Phys. Rev. B **42**, 11 530 (1990).
- ³⁹W. Jank and J. Hafner, Phys. Rev. B **42**, 6926 (1990).
- ⁴⁰J. Fisher and M. Methfessel, Phys. Rev. A **22**, 2836 (1980).
- ⁴¹J. S. Rowlinson and B. Widom, *Molecular Theory of Capillarity* (Clarendon, Oxford, 1982).
- ⁴²S. A. Rice and M. Zhao, J. Phys. Chem. A **103**, 10 159 (1999).
- ⁴³J. L. Bretonnet and N. Jakse, Phys. Rev. B **50**, 2880 (1994).